DATA BLENDING WITH ^{99m}Tc IN EVALUATING THYROID ANATOMY BY SCINTILLATION SCANNING

Harold L. Atkins and Robert F. Fleay*

Brookhaven National Laboratory, Upton, New York

Evaluating thyroid anatomy by scintillation scanning of radioactivity distributed within the gland is commonly performed with ^{131}I and occasionally with ^{125}I. Because of a rather high radiation dose to the thyroid with either of these nuclides, the amount of radioactivity administered is usually restricted to levels of 50–100 μc. Consequently counting rates are low, and the statistical reliability of the scans, if they are performed in a reasonable amount of time, is relatively poor for the fine resolution one wants.

The use of ^{99m}Tc as pertechnetate for delineating thyroid anatomy has a number of advantages. Despite the fact that less than 4% of the administered dose localizes in the thyroid in normal individuals, if one uses a 3-in.-crystal detector, counting rates 10–25 times those with ^{131}I can be obtained with equal or improved resolution (*1*). This is true because the short half-life and virtual absence of beta activity with ^{99m}Tc let one administer multimillicurie amounts, and detection and collimation of the 140-kev gamma emission is highly efficient. The 3-in.-crystal detectors are more than adequate for these studies.

Data blending is particularly suited for ^{99m}Tc in thyroid scanning for the following reasons: First, the high level of circulating radioactivity at the time of scanning can give rise to a rather high background density on the photoscan. Data blending smooths out the random distribution of densities to an even density against which any local increase in darkening can be regarded as significant. Second, elimination of the raster effect is optically more pleasing. In addition, it means that closer line spacing can be used without losing statistical reliability for a constant over-all scan time when the count density is kept constant. Therefore it is possible to take full advantage of the resolving capabilities of the collimator in two dimensions. And third, no contrast enhancement or other procedure which could result in information loss needs to be used when adequate statistical data are present.

METHOD

We reviewed thyroid scans performed with ^{99m}Tc pertechnetate on 203 consecutive individuals seen at this laboratory. The administered activity was usually 2.0–2.6 mc of ^{99m}Tc injected intravenously. Ratemeter recording of activity over the neck was continued until a steady level of counting rate was attained, usually in 10–20 min. Scanning was then started.

The instrument used for scanning is a Picker Magnascanner vacuum tube model with a 3 × 2-in. NaI(Tl) crystal. Contrast enhancement circuitry was bypassed to eliminate distortion from "scalloping" or information loss because densities in regions containing low levels of radioactivity were eliminated. The maximum speed of the detecting head had been increased from 60 to 120 cm/min. All scans were performed with the patient supine, the shoulders elevated by a pillow and the head tilted back.

A special set of collimators with 1,045 tapered holes provided increased sensitivity as well as a high degree of resolution for the 140-kev gamma emission (*2*). For thyroid scanning two collimators were used most frequently. One of these, 2.5 cm thick, has a 50% isoresponse width in air at the 8.75-cm focal distance of 0.5 cm. A 3.6-cm-thick collimator has a 50% isoresponse width of 0.4 cm. Its sensitivity is 0.6 relative to the 2.5-cm collimator. The 2.5-cm collimator is about 6 times as sensitive as the 31-hole ^{131}I collimator for an extended planar source.

The data-blending technique has been described previously (*3*). One of two Gaussian light spots, either about 8 mm or 5 mm in diameter at the 50% isodensity width, was used. Line spacing of 0.15 cm and scanning speeds of 30–60 cm/min were usually used with the maximum counting rates of 10,000–50,000 cpm. Scan time was 5–15 min, and the maximum count density was 3,600–5,400 counts/cm^2.

Revision received Jan. 27, 1967; accepted June 7, 1967.
* Royal Perth Hospital, Western Australia.

This gave a standard deviation of less than 2%—much better than is usually achieved with ^{131}I using this size detector. Uptakes were determined by a method that has been described previously (*1*).

PHANTOM STUDIES

A Lucite phantom was designed to determine the maximum resolution possible with this system and to compare data blending with conventional presentations. The central cavity measures 6.3 cm × 9.2 cm and is 2.5 cm thick. Lucite cylinders 10, 8, 6, 4 and 2 mm in diameter aligned in three rows are used to simulate "cold" nodules. One row consists of cylinders extending the entire depth of the phantom, whereas the other two rows extend only halfway with one row placed on the bottom half and the other on the top half of the phantom. A Lucite block, 6.3 × 2.5 × 1.5 cm is placed at one side of the phantom to simulate a "cool" area. The counting rate over this region was 50% of the maximum over the more active region. "Hot" nodules are introduced by drilling holes into the Lucite block. These are of the same size distribution as the "cold" nodules. The phantom is filled with water, and enough ^{99m}Tc is added to provide adequate counting statistics.

Scans were made with the count density and line spacing usually used in patient scanning. Both types of light spots were used to determine apparent magnification, and the scans were then repeated with a 20% increase and 20% decrease in scan speed to produce scans with density less or greater than optimum, respectively.

Adequate blending was determined by a homogeneous density in the areas of constant radionuclide concentration. The blended scans were composed with scans performed conventionally with a sharply marginated light spot slightly less than 3 mm in diameter. The conventional scans contained the same statistical information—the same maximum count density—as the blended scans.

TABLE 1. EVALUATION OF APPARENT MAGNIFICATION

Light spot	Scanning speed		
	Optimal	+20%	−20%
Conventional	+2 mm	+2 mm	+2 mm
Conventional (phantom angulated)	+2 mm		
5 mm blended	+1 mm	−1 mm	+1 mm
8 mm blended	+2 mm	+2 mm	+2 mm

Measurements were made across 6.3-cm axis of phantom scan at points representing 50% of maximum density.

It is apparent that in scans made with similar statistical information, the same degree of resolution is obtained with both blended and conventional scans (Fig. 1). The smallest "hot" spot seen with both scans is the 4-mm one. The 4-mm "cold" area can be identified easily when the cylinders extend through the phantom or project halfway downward from the top surface. However, cylinders extending halfway up from the bottom surface are less distinct, and the smallest one we could see easily was 6 mm in diameter. Therefore one can conclude that the resolution limit in this case is a function of the collimator rather than of the data display.

The subjective advantages of the blended scan are: (1) the borders of the phantom are more distinct, (2) the shape of the defects within are more readily discerned and (3) the regions of homogeneous activity are displayed as an even density without a superimposed "stripe" structure.

The effects of increasing or decreasing scan speed were minimal in both methods of data display. The scans performed at a speed 20% too fast were lighter and tended to show up "cold" areas better. The reverse was true for the scans performed at a speed 20% below optimum when the 4-mm "hot" nodule was more readily visible. The change in apparent size of the phantom with change in scan speed was

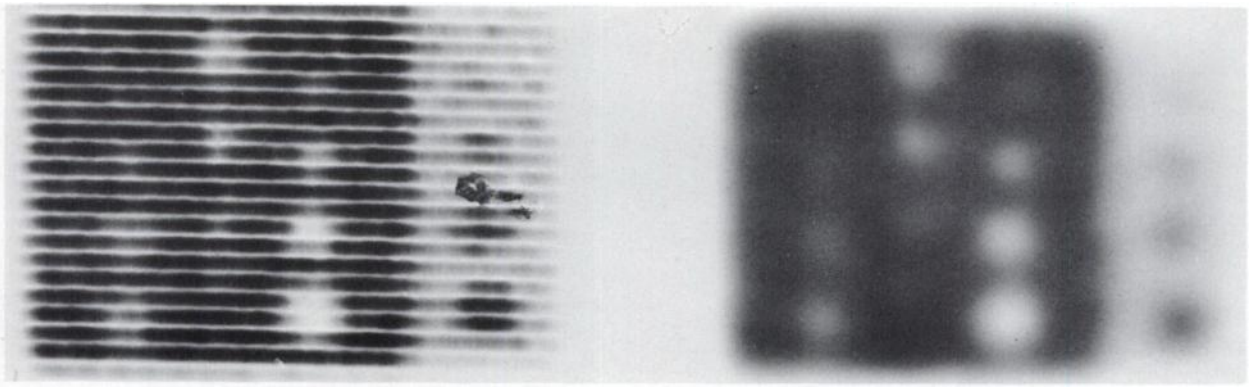

FIG. 1. Comparison of conventional scan (left) and blended scan (right) of phantom containing simulated nodules described in text. Note improved definition of margins and shape of nodules in blended scan compared with conventional scan.

TABLE 2. DISTRIBUTION OF ^{99m}Tc-PERTECHNETATE IN THYROID

	Number of patients	Visualization of isthmus	Visualization of pyramidal lobe	Discrete nodules			Diffuse heterogeneity
				Total	Functioning	Nonfunctioning	
Euthyroid	157 (89.2%)	149 (95.0%)	13 (8.3%)	17 (10.8%)	9 (5.7%)	8 (5.1%)	13 (8.3%)
Hyperthyroid	19 (10.8%)	18 (94.6%)	3 (15.8%)	3 (15.8%)	3 (15.8%)	0 (0%)	8 (42.1%)
Total	176 (100%)	167 (94.9%)	16 (9.1%)	20 (11.4%)	12 (6.8%)	8 (4.5%)	21 (11.9%)

minimal. A measurement was made along the shorter axis of the phantom scan from points representing 50% of the maximum density. The results are shown in Table 1. The apparent magnification is greater with the conventional scan than with the blended scan using the smaller light spot. The fact that scanning performed with the phantom angled away from the direction of scan motion did not change the magnification factor showed that this magnification was not caused by the discrete indexing step of 0.3 cm used with the conventional scan.

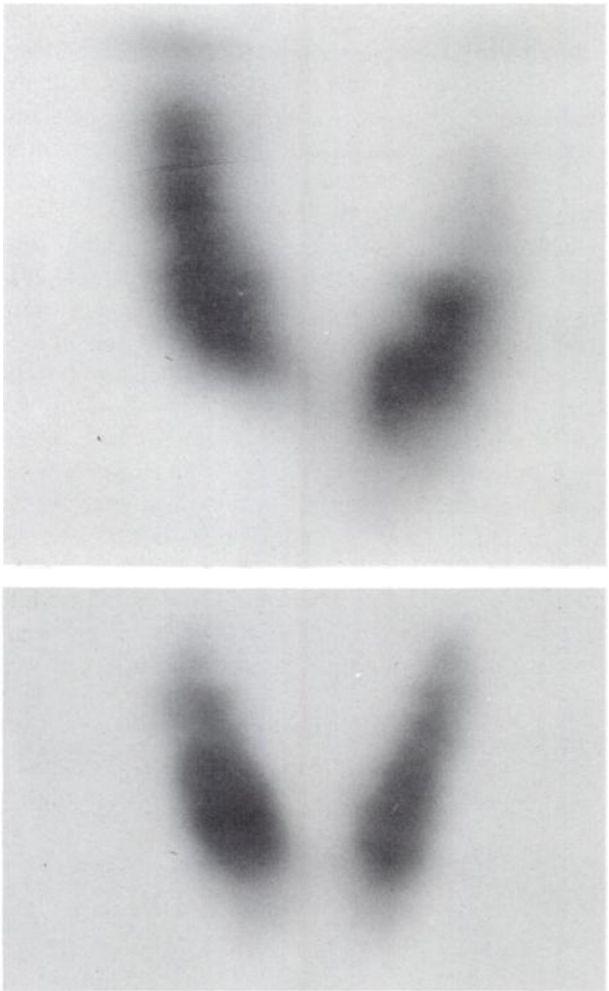

FIG. 2. Examples of diffuse heterogeneity of uptake. Patient whose scan is at top had clinical diagnosis of chronic thyroiditis (not included in tabulated series). Patient whose scan is at bottom had diffusely enlarged gland with rather high uptake of technetium (3.7%) which suppressed to 1.5%. Pattern of scan following suppression was unchanged.

RESULTS

The photoscans were analyzed for the following items: homogeneity or heterogeneity of uptake, presence of discrete nodules, shape of the poles, relative size of the two lobes and visualization of the isthmus and pyramidal lobe.

Of the 203 scans available for analysis, 176 were suitable for this study. Twenty-seven scans were eliminated because of low uptakes with indistinct borders, presence of carcinoma or thyroiditis or surgical absence of a lobe.

The background was usually discernible as a smooth light gray density on the photoscan except when the thyroidal uptake was exceptionally high. Background density varied inversely with maximum counting rate over the thyroid. Any significant density increase, even though very faint such as in a small pyramidal lobe, could be interpreted with confidence.

The 176 patients included 154 females and 22 males, a ratio of 7:1. Nineteen hyperthyroid individuals were included in this total (17 females, 2 males, a ratio of 8.5:1). The average age was 36 years.

In most patients the radioactivity distribution was homogeneous except where the gland tapered at the poles. However, in 21 patients (12%) there was a heterogeneity of uptake (Table 2) consisting of a diffuse irregularity of isotope distribution throughout the gland so that discrete nodules could not be seen (Fig. 2). These glands were usually enlarged. The heterogeneity could not be attributed to statistical fluctuations in counts because all scans were performed with the same range of count density.

FIG. 3. Technetium scans in 4 patients with hyperthyroidism. Discrete hyperfunctioning nodules appear in upper two scans. Scan on lower right shows rather heterogeneous distribution of radioactivity, and faint pyramidal lobe appears to left of midline, apparently unconnected to remainder of gland. Scan on lower left shows homogeneous distribution of radioactivity and tapering of upper poles about trachea.

Interestingly, 8 of these patients with heterogeneity of isotope distribution were hyperthyroid. Presumably the heterogeneous distribution is due to the presence either of multiple small nodules under the minimal size that can be resolved by the scanning system or to variations in physiological state throughout the gland. No pathological correlation could be obtained in any of these cases.

Discrete single or multiple nodules were noted in 20 patients (11%) over-all and in 17 of the euthyroid patients (11%) (Figs. 3 and 4). In the 3 hyperthyroid individuals these were hyperfunctioning nodules. In the euthyroid individuals these were nonfunctioning in 5 and functioning in 12. However, in only one patient was autonomy of the nodule demonstrated by a TSH suppression test (Fig. 5). The diagnosis of functioning nodules was somewhat subjective. Many patients had what we considered regions of thickening of the gland with a consequent higher counting rate over these areas. We tended to be conservative in our estimate of what constituted nodularity, basing the diagnosis on the shape of the functioning area and its relationship to the remainder of the gland.

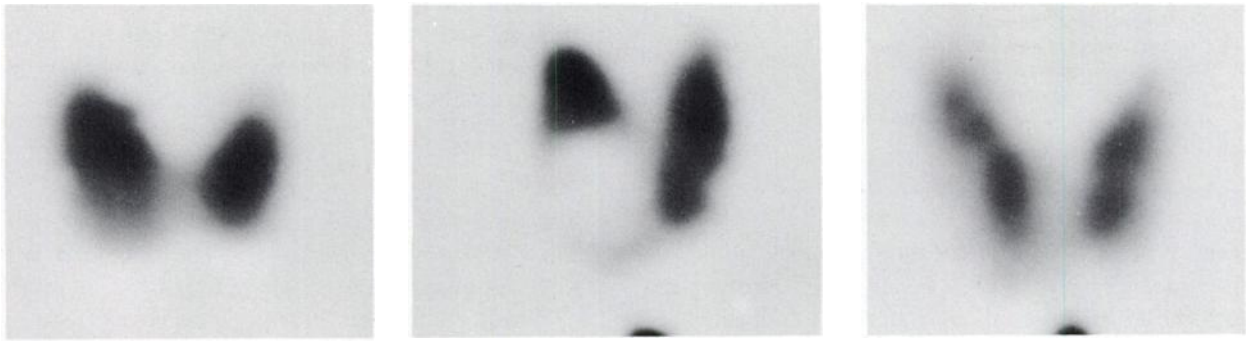

FIG. 4. Nonfunctioning nodules. Scan on left shows about 50% reduction in activity over right lower pole at palpable nodule. In middle scan signet-ring-like deformity is created by large cystic nodule in right lobe. In right-hand scan multiple areas of diminished uptake are seen, some poorly defined, in addition to palpable nodule along lateral border of right lobe.

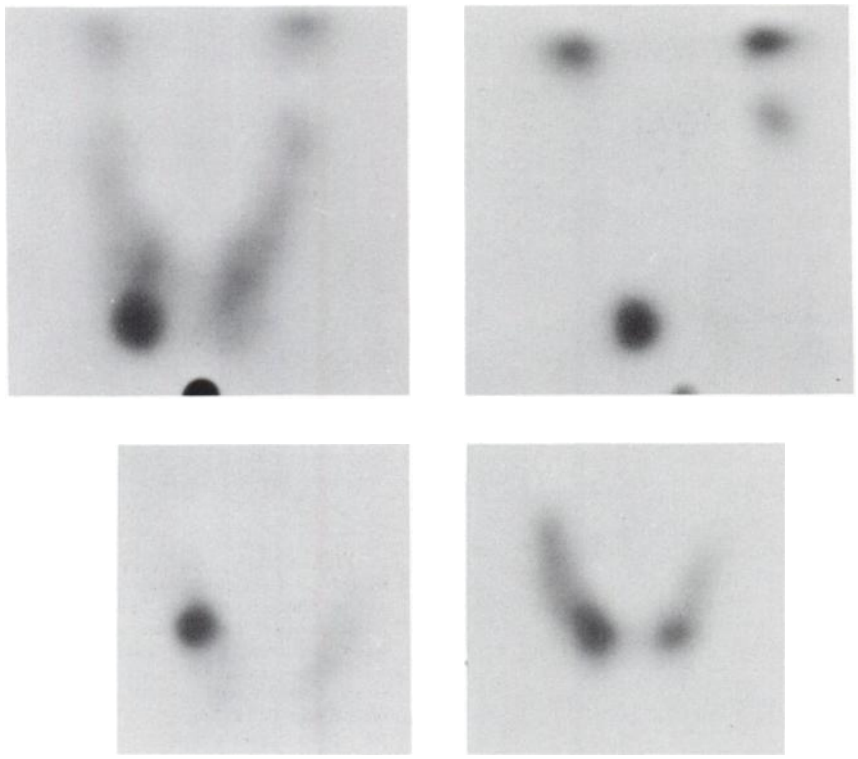

FIG. 5. Upper scans are on patients before (left) and after (right) TSH suppression with l-triiodothyronine. Palpable functioning nodule in right lower pole is unsuppressed. However, additional functioning nodule at left upper pole, unsuspected in presuppression scan, can be seen in postsuppression scan. Note lack of suppression in salivary glands at top of scan. Left lower scan shows hot nodule in right lobe. Pathological diagnosis was hyperplastic adenoma. Right lower scan shows increased density at both lower poles, interpreted as thickening of gland rather than presence of nodules.

A number of patients with palpable discrete nodules showed no abnormalities on the scan for two reasons: Some of the nodules were too small (less than 4 mm in diameter) to be resolved by isotopic means. In addition, unless the nodule displaced normally functioning tissue, it would not be discernible.

Other interesting variations in anatomy are listed in Table 3. These included rounded or tapered inferior poles and tapering of the upper pole about the trachea and larynx (Figs. 6 and 7). Determination of some of these variations was rather subjective because many degrees of tapering exist. In only one patient in this series was there any substernal component to the thyroid. The isthmus was visualized in 95% of all individuals, euthyroid and hyperthyroid alike. A pyramidal lobe was seen in 13 euthyroid individuals (8.3%) and in 3 hyperthyroid individuals (15.8%). It was usually separated from the main portion of the gland and was frequently to one side of the midline (Fig. 8). The true incidence of pyramidal lobe is probably considerably higher, but a relative lack of function makes it difficult to detect on the scan.

TABLE 3. ANATOMICAL VARIANTS IN THYROID SCANS

Total number of patients: 176	
Both lower poles rounded	132 (75.0%)
Both lower poles tapered	15 (8.5%)
Right lower pole tapered	21 (11.9%)
Left lower pole tapered	8 (4.5%)
Upper poles tapered about trachea	84 (47.7%)
Right lower pole lower than left	34 (19.3%)
Right lower pole higher than left	48 (27.3%)
Right and left lower poles at same level (±2 mm)	94 (53.4%)

Only rarely was the thyroid truly symmetrical. Most often (77%) the right lobe was larger (Table 4). The opposite was true 18% of the time, and in only 5% of the cases was there less than a 3-mm difference in length between the two lobes. On the average, the right lobe was 17% longer and 9% wider than the left lobe. While the lower border of both lobes was at the same level (±2 mm) in 53% of the cases, the right lobe was higher more often if any discrepancy existed.

DISCUSSION

The results of this study confirm previous reports of the relative thyroid asymmetry. The right lobe was more often larger than the left as found by Thomson (*4*), and the difference in size of the lobes, as well as their average dimensions, are remarkably close to the values found by Spencer and Waldman (*5*) using ^{181}I.

TABLE 4. COMPARISON OF LOBE SIZE IN 157 EUTHYROID INDIVIDUALS

	Mean (cm)	Standard deviation	Greatest (cm)	Least (cm)	Average error	Possible error	Coefficient of variation
Length of right lobe	4.9	±1.03	7.5	2.2	0.82	0.7	0.21
Length of left lobe	4.2	±1.03	9.7	1.6	0.82	0.7	0.25
Width of right lobe	2.1	±0.42	3.6	1.2	0.33	0.3	0.20
Width of left lobe	1.9	±0.37	3.4	1.0	0.29	0.3	0.20

Right lobe on average is 17% longer and 9% wider than left.
Right lobe greater than left lobe by 3 mm or more in length in 121 cases (77.1%).
Left lobe greater than right lobe by 3 mm or more in length in 28 cases (17.8%).
Right lobe equal to left lobe in 8 cases (5.1%).
Rank correlation coefficient between length of right and left lobes is 0.97.

The data-blending type of scan presentation makes it possible to delineate borders more clearly than with the conventional type of photoscan. In addition, the more subtle shadings and tapering of the poles of the gland are more readily appreciated. By avoiding contrast enhancement, one can visualize the isthmus and small pyramidal lobes which might be missed easily otherwise. Elimination of the "raster" effect and of the random background densities is extremely helpful. While detector resolution is unchanged with this method, the perception limits in visual appreciation of the scans is much improved.

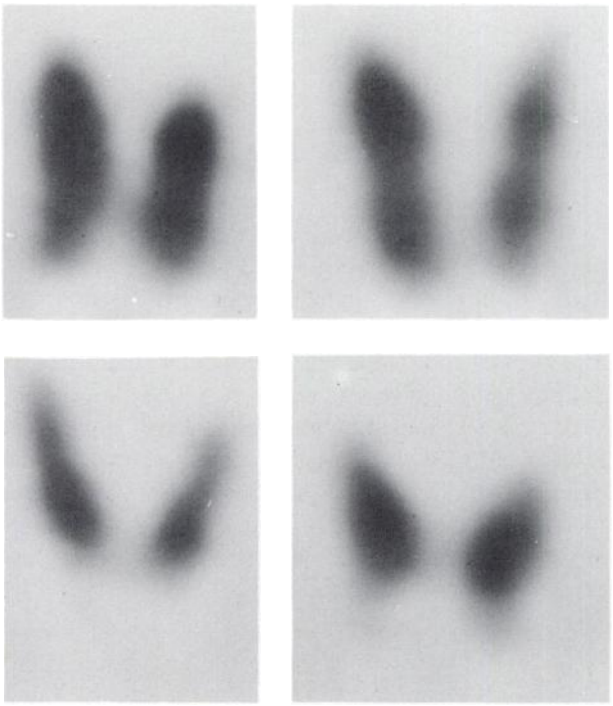

FIG. 6. Variations in thyroid shape. Note faint tapering of lower pole in bottom two scans.

While it can be shown mathematically that there may be some loss of resolution with data-blending (*6*), this was not apparent in our phantom studies, and the advantages in pattern recognition with this type of presentation outweigh any disadvantages. It has been shown that "noise" can prevent perception of what would otherwise be a readily perceptible pattern (*7*). Random background densities and the horizontal stripes of the raster constitute "noise" which disrupts the scan pattern and obscures important detail and subtle shadings from one region of the thyroid to adjacent regions.

With or without data blending, an apparent magnification of the gland may be produced if the activity of the gland is not in the focal plane of the collimator or if the photorecording sensitivity is too high, producing increased blackening. Despite these possibilities, the average figures obtained in this series offer very good comparison with those obtained by Spencer and Waldman.

An apparent size reduction can be produced by contrast enhancement methods or by too light a photoscan. We feel that too much information can be lost by introducing contrast enhancement. With the high statistical accuracy obtained with ^{99m}Tc scanning, no contrast enhancement is required. A just-visible background density on these scans is assurance that no significant functioning regions are missed, and statistically significant counting-rate changes are perceived easily in the resultant density variations on the scan. On the basis of our phantom studies we feel that our measurements are reasonably accurate.

The incidence of nodules in this series is similar to that found in other series, but comparison cannot be made because of differences in patient selection.

FIG. 7. Examples of tapering of upper poles about trachea. Note asymmetry of two lobes and—in central scan—nonfunctioning nodules.

A very high proportion of our cases was scanned during a work-up for evaluation of function rather than for thyroid enlargement or nodules. The presence of a rather high number of hot nodules is somewhat unusual. It is possible that these hot nodules would have been missed with conventional scanning methods. This is certainly true in one of our cases where scans were performed with both methods (Fig. 9). It is unlikely that the use of ^{99m}Tc rather than ^{131}I is responsible for this, because the distribution of activity has been identical in the few cases where we have used both nuclides. To rule out the possibility that the use of data blending or technetium is responsible for this unusual number of functioning nodules, it would be necessary to scan all cases with ^{131}I and ^{99m}Tc both with conventional data recording and with data blending. This was not practical for us to do with all patients in this series.

Almost certainly more nodules exist than can be discovered by scintillation scanning. Mortensen, Woolner and Bennett (*8*) have shown that about 50% of thyroids in a large series of autopsies on patients with presumably normal glands had nodules. More than a third of these nodules were larger than 2 cm, yet had not been detected clinically. Nodules must be large enough to produce a significant change in counting rate and must be in a location where normally functioning tissue is displaced or replaced before they can be visualized on the scan. Another requirement for detection is that the functional state of the nodules should be significantly different from the rest of the gland. In one case one hot nodule did not become apparent until after TSH suppression reduced uptake in the normal portion of the gland (Fig. 3).

Undoubtedly greater accuracy could be achieved by using magnetic tape and computer processing to record all information. Playback at different cut-off levels, and with statistical fluctuations averaged out, would result in greater informational content. Unfortunately this equipment is not generally available today and is out of the reach of many community hospitals because of cost and the complexity of equipment. However, the method used to produce our scans is within reach of any radioisotope laboratory and is readily reproducible with only minor modification of most available equipment.

SUMMARY

We have included the assessment of thyroid anatomy using scanning with ^{99m}Tc pertechnetate and a data-blending technique in 176 patients. Several features such as isthmus visualization, the presence of a pyramidal lobe, tapering of the poles, incidence of nodules and relative size of the two lobes were tabulated. We feel that the data-blending technique used in association with the high counting rates and low patient radiation doses possible with this method increase the accuracy of thyroid scanning by improving the pattern presentation and allowing easier perception of anatomical variations.

ACKNOWLEDGMENT

This research was supported by the U.S. Atomic Energy Commission.

REFERENCES

1. ATKINS, H. L., AND RICHARDS, P.: Assessment of thyroid function and anatomy with technetium-99m as pertechnetate. *J. Nucl. Med.* **9**:7, 1968.

2. RICHARDS, P. AND ATKINS, H. L.: A collimator system for scanning at low energies. *J. Nucl. Med.* **8**:143, 1967.

3. ATKINS, H. L.: Practical modifications of the rectilinear scanner. *Am. J. Roentgenol. Radium Therapy Nucl. Med.* **97**:888, 1966.

4. THOMSON, J. A.: The normal thyroid scan. *Lancet II:* 308, 1966.

5. SPENCER, R. P. AND WALDMAN, R.: Size and positional relationships between thyroid lobes in the adult as determined by scintillation scanning. *J. Nucl. Med.* **6**:53, 1965.

6. FREEDMAN, G. S., WOLBERG, J. R. AND JOHNSON, P. M.: Information content of conventional and data-blended photoscanning. *Radiology* **88**:345, 1967.

7. JULESZ, B.: Texture and visual perception. *Sci. Am.* **212**:38, 1965.

8. MORTENSEN, J. D., WOOLNER, L. B. AND BENNETT, W. A.: Gross and microscopic findings in clinically normal thyroid glands. *J. Clin. Endocrinol. Metab.* **15**:1,270, 1955.

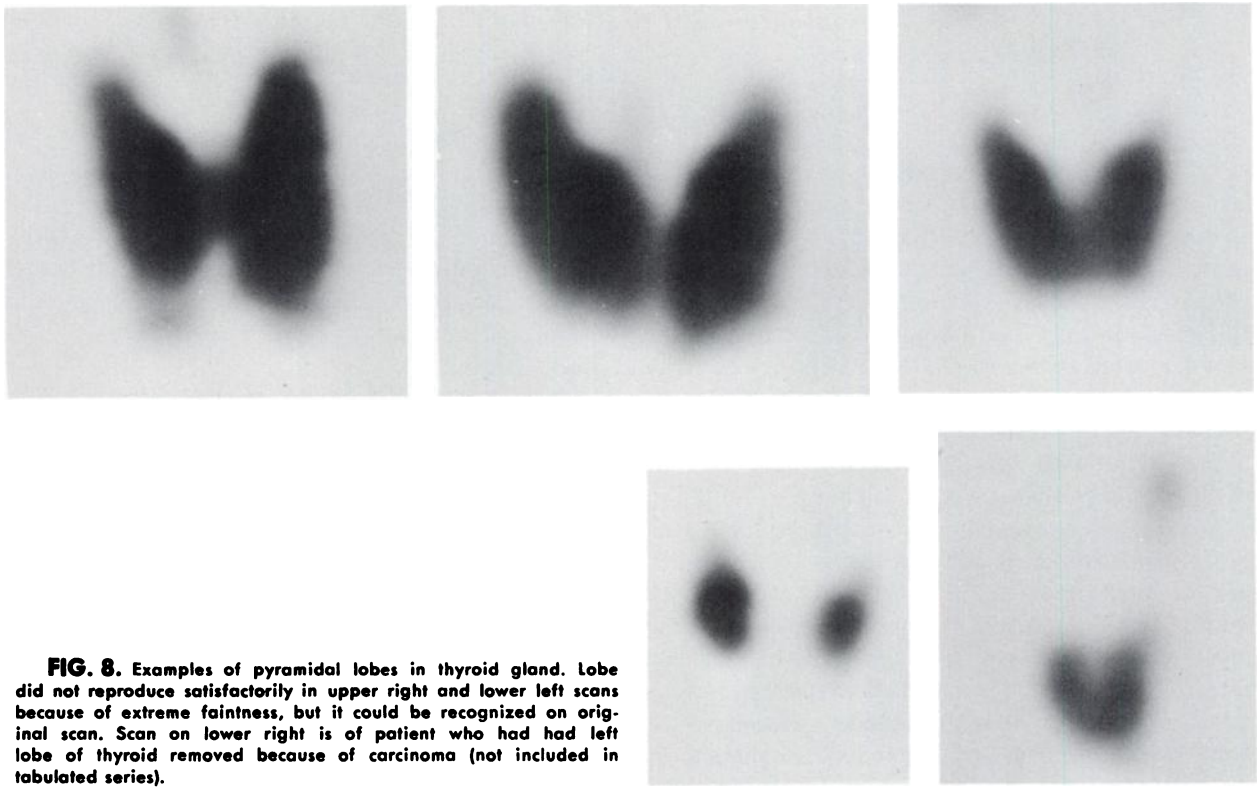

FIG. 8. Examples of pyramidal lobes in thyroid gland. Lobe did not reproduce satisfactorily in upper right and lower left scans because of extreme faintness, but it could be recognized on original scan. Scan on lower right is of patient who had had left lobe of thyroid removed because of carcinoma (not included in tabulated series).

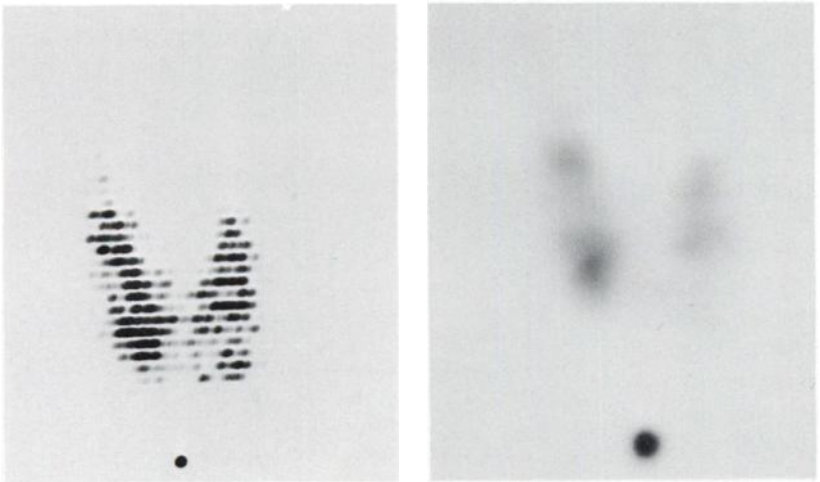

FIG. 9. Series of scans in one patient to demonstrate value of data blending. Scan on far left was performed 24 hr after oral administration of 50 μc ^{131}I. With conventional presentation, appearance is that of multiple cold nodules. Data-blended scan (near left) made on same day reveals multiple hot nodules. ^{99m}Tc scan performed with data blending (below) shows more clearly physiological and anatomical character of gland.